doi:10.1007/s11589-011-0815-1

The synergy of earthquake precursors*

Sergey Pulinets[1,2,♣]

[1] *Fiodorov Institute of Applied Geophysics, Moscow* 129128, *Russia*
[2] *Space Research Institute, Russian Academy of Sciences, Moscow* 117997, *Russia*

Abstract The system of geophysical shells (lithosphere, atmosphere, ionosphere) is considered as an open complex nonlinear system with dissipation where earthquake preparation could be regarded as a self-organizing process leading to the critical state of the system. The processes in atmosphere and ionosphere are considered from the point of view of non-equilibrium thermodynamics. The intensive ionization of boundary layer of atmosphere (probably provided by radon in occasion of earthquake preparation) gives start to the synergetic sequence of coupling processes where the ionosphere and even magnetosphere are the last links in the chain of interactions. Every anomaly observed in different geophysical fields (surface temperature, latent heat flux, electromagnetic emissions, variations in ionosphere, particle precipitation, etc.) is not considered as an individual process but the part of the self-organizing process, the final goal of which is the reaching of the point of the maximum entropy. Radon anomaly before the Kobe earthquake is considered as a perfect example to satisfy the formal seismological determination of the earthquake precursor. What is genetically connected with radon through the ionization process can also be regarded as a precursor. The problem of co-seismic variations of the discussed parameters of atmosphere and ionosphere is considered as well.

Key words: **synergy; earthquake precursor; complex system; radon; entropy; critical state**
CLC number: P315.72 **Document code**: A

1 Introduction

The problem of short-term earthquake prediction counts many years of history, but still the relation to this problem is more negative (especially among seismologists, Geller et al., 1997) and all attempts to present the results indicating the connection of observed geophysical anomalies with the approaching earthquake meet negative attitude in seismological community. But orthodox position of Geller is not fully accepted by seismologists as a whole. I would like to cite Max Wyss (1997a) from Geophysical Institute, University of Alaska: "At the time of Columbus, most experts asserted that one could not reach India by sailing from Europe to the west and that funds should not be wasted on such a folly. Geller et al. make a similar mistake ..." Negativism directed to the precursory science is not only due to conservatism of seismology but also because of many speculative publications appeared during last decades, and inability to demonstrate that observed anomalies conform to the formal determination of precursor (Wyss, 1997b). Majority of anomalies pretending to be nominated as precursors demonstrate the ability to "predict" only one or two from three main earthquake parameters (time, place, magnitude), and do not usually demonstrate clear indication of approaching to the critical state, and very often miss the co-seismic signal which is considered very important signature of relation of the observed anomaly with the approaching seismic shock.

From the other side the counterarguments could be put forward. One can observe very slow progress in development of the physics of earthquake preparation, inability of seismology to describe in the physical language the processes happening in the Earth's crust during the seismic cycle (from previous to the next earthquake at the same focal area), what might give to scientists possibility to explain the observed anomalies, named earlier the physical precursors of earthquakes (Scholz et al., 1973). We should agree with Dobrovolsky (2009) that earthquake prediction is the reversed problem of the

* **Received** 10 October 2011; **accepted in revised form** 5 November 2011; **published** 10 December 2011.
♣ **Corresponding author. e-mail**: pulse1549@gmail.com

physical mechanism of earthquake preparation.

This paper attempts to find a reliable compromise between different points of view using both the formal seismological approach to precursors and their physical nature, which is connected with the development of critical state of the complex system during earthquake preparation. The recent developments of lithosphere-atmosphere-ionosphere coupling (LAIC) model (Pulinets and Ouzounov, 2011) have demonstrated that the observed anomalies within the time interval few days before the seismic shock are not the set of independent variations of different geophysical parameters just like it is considered in different publications (Cicerone et al., 2009) but demonstrate some synergy in their behavior, space and time synchronism, nonlinearity. Existence of different thresholds leading to the qualitative change in the system states, presence of different phases of the same substance (water) participating in interaction, multi-scale dynamics led to conclusion of synergetic character of the observed phenomena. Recent publications (De Santis et al., 2011) give understanding of the direction of the process development based on the maximum entropy approach, and more chances to include the pre-seismic anomalies into the family of earthquake precursors.

Taking into account that radon plays the crucial role in the LAIC mechanism, essential part of the paper is devoted to the substantiation of precursory nature of radon variations before earthquakes. The consequences of radon action on atmosphere, which is ionization of boundary layer, can also be regarded as precursor using their physical nature and genetic coupling with radon.

2 Exoneration of radon as earthquake precursor

According to Wyss (1997b) the earthquake precursors should satisfy the well-determined formal criteria:

Validation criteria. Proposed precursors should satisfy the following criteria: (1) The observed anomaly should have a relation to stress, strain, or some mechanism leading to earthquakes. Evidence of a relationship between the observed anomaly and the mainshock should be presented; (2) The anomaly should be simultaneously observed on more than one instrument, or at more than one site; (3) The amplitude of the observed anomaly should bear a relation to the distance from the eventual mainshock. If negative observations exist closer to the mainshock hypocenter than to the positive observations, some independent evidence of the sensitivity of the observation sites should be provided. For instance, if the anomaly is observed at a site that appears particularly sensitive to precursory strain, it should also be more sensitive to tidal and other strains; (4) The ratio of the size (in time and space) of the dangerous zone to the total region monitored shall be discussed to evaluate the usefulness of the method.

We leave out the scope of this paper the questions of data quality, anomaly detection, and association with subsequent earthquakes. Our main concern would be the *Validation criteria*. We will also keep the physical principle that if the relationship is established, it will be fulfilled for other cases because of universal character of the physical laws. The Kobe earthquake case (Japan, 17 Jan. 1995, M_W6.9, 05:47 JST, strike-slip focal mechanism) is selected for consideration as the most carefully analyzed (Yasuoka et al., 2010).

Actually, the radon-stress connection was considered in many papers, starting from Roelofs (1998) where radon and strain data for the M7 Izu-Oshima earthquake of 14 January 1978 show changes preceding the earthquake and synchronous sharp changes with approaching the main shock. Regardless the earthquakes, the radon variations associated with the Earth's crust deformation were reported in Triqué et al. (1999) for the case of deformation produced by reservoir water level, in Aumento (2002) for the high correlation of solar tides and radon variations. Šebela et al. (2010) analyzed the 3D deformations in cave and their direct correlation with radon variations.

But the most interesting for our consideration is the results presented in Yasuoka et al. (2006) where atmospheric radon variations and the close proximity to the Kobe earthquake epicenter are considered using the critical point conception. Figure 1 demonstrates the best fit of the residual of air radon variations with a log-periodic power law as typically used for the cumulative Benioff strain (Sornette and Sammis, 1995). Main conclusion of the paper is that the power-law of the Benioff strain (Ben-Zion and Lyakhovsky, 2002), and the log-periodic oscillation model (Sornette and Sammis, 1995), are applicable to not only Benioff strain, but also to atmospheric ^{222}Rn change. This result immediately brings us to conclusion that radon variations before Kobe earthquake perfectly satisfy the item (1) of *Validation criteria*.

From collection of papers regarding the radon variation analysis before the Kobe earthquake (Yasuoka et al., 2010) it is possible to find that the radon measurements were carried out by two different techniques

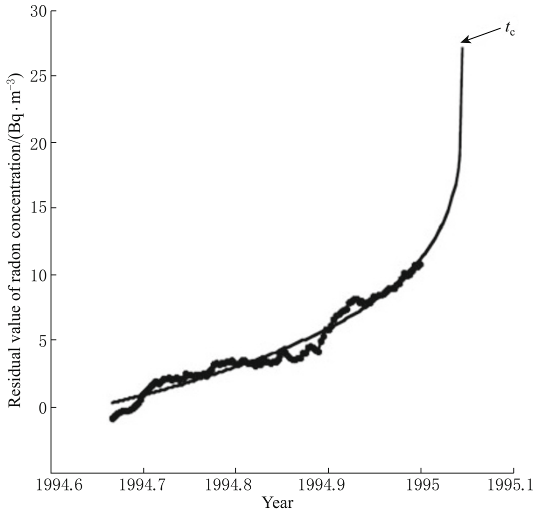

Figure 1 Variations of the analytical smoothed residual ^{222}Rn concentration (closed circles) and the log-periodic best fit curve of the critical exponent (Sornette and Sammis, 1995) for the fixed t_c=1995.045 (t_c is the time when the system reaches the critical point). An arrow indicates the critical point. After Yasuoka et al. (2006).

giving data of air radon variations and radon concentration in water (Yasuoka et al., 2009). Both show the variations with relation to strain and sharp increase while approaching the critical point. We can conclude that radon variations before Kobe earthquake also satisfy the item (2) of *Validation criteria*.

Considering the item (3) we should turn to the statistical data, best presentation of which concerning radon variations are given in Toutain and Baubron (1998). This comprehensive review shows that radon follows the logarithmic distribution in relation to distance from epicenter versus magnitude, first formulated by Dobrovolsky et al. (1979) (see Figure 2). From Figure 2a one can see magnitude-distance relations for different levels of elastic deformation. By different symbols are marked different anomalies (crust conductivity, magnetic, gravimetric, seismic velocity, etc.) registered at the maximal distance from the epicenter of earthquake of given magnitude. It is clearly seen that they are concentrated near the line corresponding to the 10^{-8} deformation level. Figure 2b (Toutain and Baubron, 1998) shows the similar distribution only for radon. It demonstrates that majority of the points are situated under the line also corresponding to the deformation 10^{-8}. The authors used not only the maximum distance from the epicenter, but all points, that is why they are spread in the space below the line of 10^{-8}. Dobrovolsky in his recent publication (Dobrovolsky, 2009) interpreted the limit 10^{-8} as a level which tide deformations can reach, so everything that is higher than 10^{-8} would be connected with stronger deformations associated with tectonic activity. But this relation has more profound meaning connected with the reaching the system of critical state (Bowman et al., 1998). In the discussion they proposed, "that the critical region is controlled by the size of the regional fault network, rather than by the transfer of

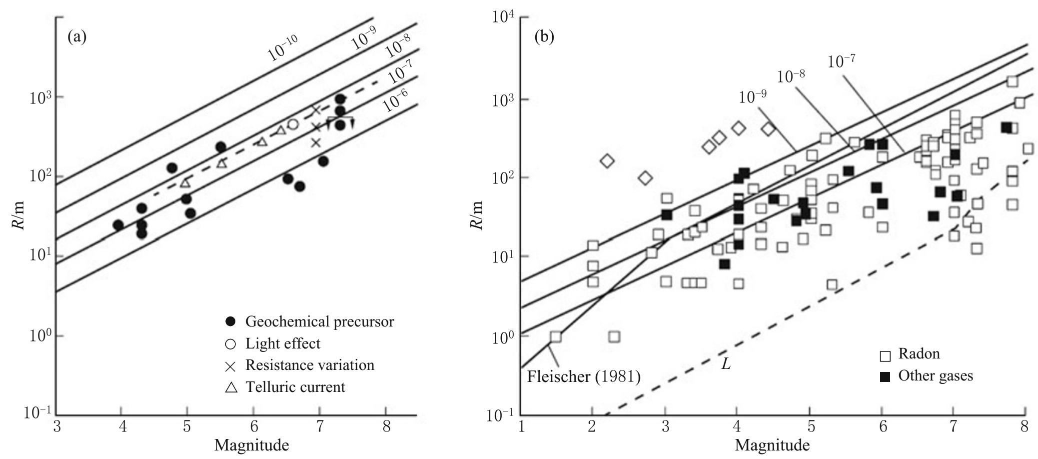

Figure 2 (a) Determination of the size of earthquake preparation zone in relation to magnitude according to Dobrovolsky et al. (1979). (b) Radon and geochemical precursors of earthquake distribution versus magnitude according to Toutain and Baubron (1998). The single bold line characterizes the empirical relationship of Fleischer (1981) who calibrated the maximum distance of a radon anomaly for a given magnitude on the basis of a shear dislocation of an earthquake. Dashed line L characterizes typical rupture length of active faults as a function of magnitude by using the empirical law of Aki and Richards (1980). Modified from Pulinets et al. (2004).

elastic energy to the fault plane". They considered the proportionality between the size of the largest member in the fault system L and the radius of the critical zone R, and concluded that in practice, R can be ten times larger than L or more. Using results of Kanamori and Anderson (1975) they obtain

$$\log R \sim 1/2M. \quad (1)$$

But the best fit gives the value of slope 0.44 which is almost the same as 0.43 of Dobrovolsky et al. (1979), $R=10^{0.43M}$. So we can interpret the relation shown in Figure 2 as determination of the critical zone size which is equivalent to the earthquake preparation zone.

It should be noted that formulation of item (3) of *Validation criteria* is a little bit straightforward and primitive if taking into account the complexity and heterogeneity of earthquake preparation region. Direct amplitude versus distance relationship for precursor appearance could be observed only for ideal elastically deforming media. There is also not a direct coincidence of the point of the maximum strain and focal zone. Earthquake happens in the weakest point of the critical area, which is not necessarily the point of the maximum strain. It is clearly seen from Figure 3 (Ouzounov et al., 2005) where the thermal anomalies are stronger over active tectonic faults than in the vicinity of epicenter (shown in figure by asterisk).

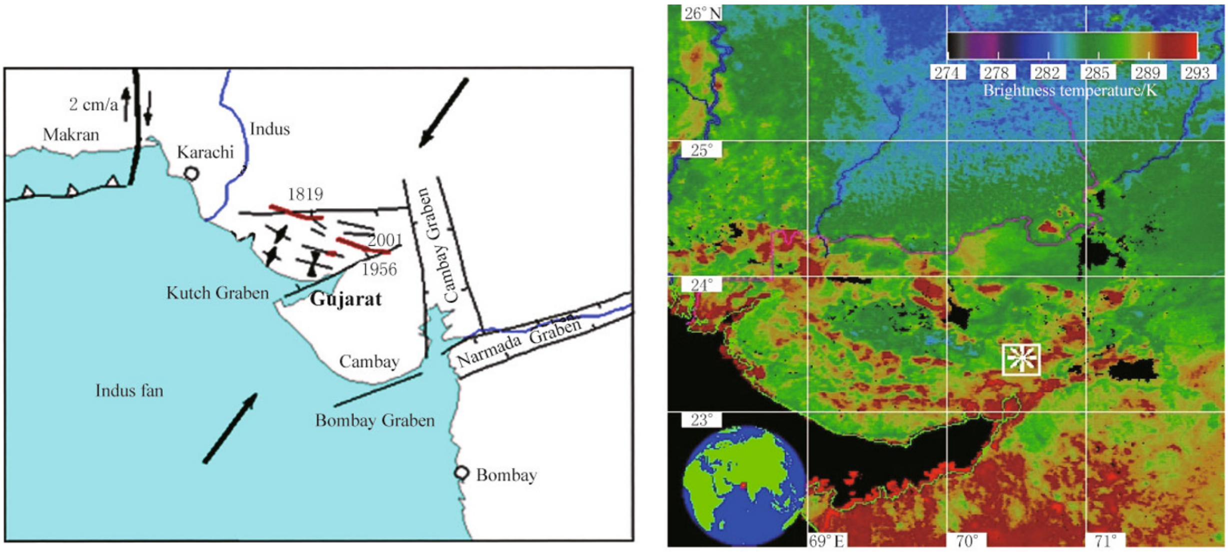

Figure 3 (a) Tectonic map of India. (b) Thermal anomalies observed six days before the Gujarat earthquake M7.9 on 26 January 2001. After Ouzounov et al. (2005).

The item (4) of *Validation criteria* has practical sense only for small earthquakes because for earthquakes with $M>7$ the "dangerous zone" or by other definition, earthquake preparation zone may cross the state borders. Here two extreme cases could be mentioned. For Sumatra-Andaman earthquake of 26 December 2004, the earthquake preparation zone was 7 000 km, and it is worth speaking about the global network of earthquake precursors monitoring. It should also be mentioned that for this earthquake the anomalous radon variations were registered at West Bengal province of India (Das et al., 2005). From the other point the only one country in the world where radon monitoring is organized using uniform grid of observations based on unified technology is Turkey where criterion (4) could be satisfied in terms that earthquake preparation area would be smaller than the whole observation network.

Concluding the paragraph, we can state that the dignity to be named "earthquake precursor" could be returned to radon, which means that its regular observations should be re-established in the seismically active zones of our planet, which really happens. The number of publications on radon anomalies before earthquakes has been growing exponentially during the last few years, confirming its validity to be used in the earthquake prediction problem (İnan et al., 2008; Šebela et al., 2010). It would be logical (from the physical point of view) to consider all other processes in atmosphere, which are the consequence of anomalous radon fluxes action onto atmosphere also as earthquake precursors.

3 LAIC model as a complex system

The lithosphere-atmosphere-ionosphere coupling model started its development in 1998 (Pulinets et al., 1998), and through several modifications (Pulinets et al., 2000, 2002, 2006; Kim et al., 2002; Pulinets and Boyarchuk, 2004) it reached its completeness quite recently (Pulinets and Ouzounov, 2011). What this model differs from many others lies in its multidisciplinary character involving seismology, geochemistry, atmospheric chemistry, meteorology, thermodynamics, atmospheric electricity, plasma physics, space plasma electrodynamics, etc. The processes described by the model are developed in different geophysical shells starting from the Earth's crust, through atmosphere, ionosphere, up to magnetosphere. To track the development of anomalies with approaching the earthquake moment we have to measure (or to model) many different parameters of different geophysical media which put forward the idea of multiparametric approach in earthquake precursors monitoring. The model demonstrates its essentially nonlinear character having different thresholds in processes development and characteristic branch points. And what is most important, the processes development has some kind of directionality, intrinsic to the complex chaotic processes leading to the critical state of the system. This property is inherent for the most of natural irreversible processes (especially in biology), and is named as "time's arrow" (Eddington, 1928). In thermodynamics (which has essential contribution to our model) the directionality of processes is described by the velocity of entropy growth (Kondepudi and Prigogine, 1998). As concerns the seismology, the similar approach was proposed recently for interpretation of b-value of Gutenberg-Richter law in terms of entropy maximum (De Santis et al., 2011). In these terms the 2009 L'Aquila earthquake was determined as chaotic process (De Santis et al., 2010).

To not rehearse the model description from Pulinets and Ouzounov (2011), we will make accent here only on features, which demonstrate the synergy of different processes — interaction of subsystems leading to simultaneous entropy growth and self-organization. We can separate the precursors generation system by several subsystems, namely: (1) radon migration in crust and exhalation into atmosphere (we will name it RN); (2) boundary layer ionization by radon and ion clusters formation through the process of ion induced nucleation (IIN); (3) latent heat release due to water vapor condensation on ions (LH); (4) changes in atmospheric electricity through conductivity changes due to ion clusters formation and interaction with aerosols (AE); (5) thermodynamic processes leading to formation of anomalous fluxes of latent heat and spots of OLR — outgoing longwave radiation (THD); (6) changes in atmospheric parameters such as surface air temperature, relative humidity, air pressure, earthquake clouds formation, jet streams (MET); (7) ionospheric effects (anomalous variations of plasma concentration and temperature), ion composition changes, optical emissions, ELF-VLF noises, coupling with magnetosphere and particle precipitation (IMC); (8) radio wave propagation effects — VLF, HF, VHF frequency bands through the changes of atmosphere and ionosphere parameters (RWP); (9) generation of electromagnetic emissions in different frequency bands — ELF, VLF, VHF (EME).

Instead of flow chart diagram of LAIC presented in Figure 10 of Pulinets and Ouzounov (2011), we propose here the multisystem conception in geophysics (Geosystemics), which is developing fast now (De Santis, 2009), and model verification and validation approach (Thacker et al., 2004), which uses the multisystem for the model's verification and validation. Using this, the LAIC can be presented as a complex graph (Figure 4) with division by subsystems mentioned above, every of which is split into the components, where every of components consists of several unit problems. It should be noted that components of subsystems may belong to several subsystems partly or completely, and this provides the complex interaction between the subsystems. As an example of such component the formation of large (aerosol size) ion clusters can be brought. It plays an important role in at least seven subsystems: (1) it is final product of the IIN subsystem; (2) formation of large ion clusters leads to latent heat release (LH) due to vapor condensation on ions; (3) large ion clusters decrease the boundary layer conductivity, changing the local parameters of the global electric circuit in the subsystem (AE); (4) large ion clusters change radiative parameters of boundary layer, modifying its thermodynamic properties (THD); (5) large ion clusters could serve as nucleus for the EQ clouds formation (MET); (6) large ion clusters through the air conductivity changes modify the conditions for subionospheric propagation of VLF signals, creating the VLF propagation anomalies; simultaneously these clusters can form the aerosol layers which serve as reflective screen for VHF signals overhorizon propagation (RWP); (7) aerosol layers through their electrification can generate the electric discharges which are registered as pulsed emission at wide frequency band (for example P-H pulses), the rotational oscillations of the complex ions can emit the continuous VHF emission also registered before earthquakes (EME).

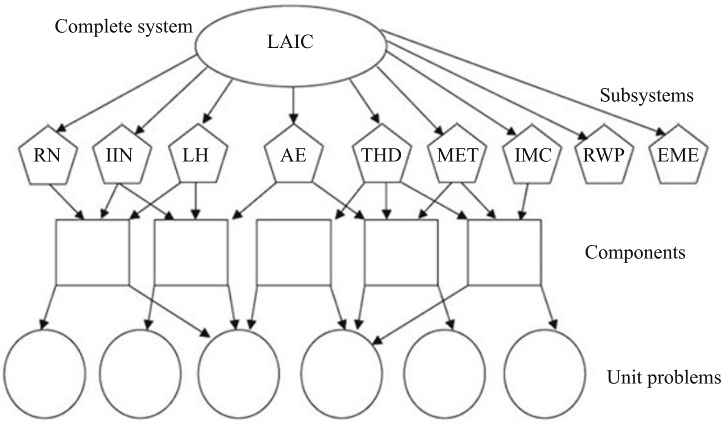

Figure 4 LAIC as a complex system (modified from Thacker et al., 2004).

As examples of unit problems we can bring calculation of ion concentration as a result of ionization by radon and its progenies, or calculations of air conductivity changes, or estimation of latent heat released, etc.

It should be mentioned that subsystems interact through their components creating the positive and negative feedbacks. For example, the high air relative humidity facilitates the formation of large ion clusters in IIN process, but intensive condensation of water vapor on ions will decrease the relative humidity. And these feedbacks automatically lead to the existence of different thresholds in the system, which may bring the ambivalent results. The size and stability of ion clusters, which are formed under IIN process, depend mainly on ion concentration and relative humidity (Pulinets et al., 2006). The initial phases of IIN are described in Yu and Turco (2001) while considering the troposphere ionization by galactic cosmic rays. One can find different versions of IIN models (Laakso et al., 2002). In Pulinets et al. (2006) was shown that in phase transitions of water vapor the latent heat for the water molecule is equal to its chemical potential or work function to separate the molecule from the water drop. In the multicomponent media with external impact, relative humidity H can be expressed as

$$H(t)=\frac{\exp(-\dfrac{U(t)}{kT})}{\exp(-\dfrac{U_0}{kT})}=\exp\left(\frac{U_0-U(t)}{kT}\right)=$$

$$\exp(-\frac{0.032\Delta U\cos^2 t}{(kT)^2}), \qquad (2)$$

where $U(t)=U_0+\Delta U\cdot\cos^2 t$, ΔU is the averaged by the volume chemical potential correction as a result of external impact. The daily variations of the solar radiation were taken into account as cosine quadrate. It is also taken into account that U_0 was calculated for the boiling temperature. The ΔU is the integrated factor reflecting the process of ion clusters formation. The larger ΔU the larger the bond energy of water molecules, the more stable are ion clusters (longer living time before recombination), the larger size they can reach. The spectrum of ion size in the Earth's atmosphere is now extensively studied (Hõrrak et al., 1998; Hirsikko, 2011). Experimental measurements show the wide variety of sizes of atmospheric ions. It is also demonstrated that ions accelerate the water vapor condensation and are very good centers for condensation (Laakso et al., 2003; Svensmark et al., 2007). At the same time it was demonstrated in experiments with coronal discharge under atmospheric pressure that size of the formed ion clusters almost linearly depends on the relative humidity (Sekimoto and Takayama, 2007).

It is well established also that ion cluster size is important for the boundary layer electric conductivity because of different mobility of ions with different size (Hõrrak, 2001). According to this publication the mobility for different ions varies in normal conditions from 3.14 $cm^2\cdot V^{-1}\cdot s^{-1}$ for small ions to 4.1×10^{-4} $cm^2\cdot V^{-1}\cdot s^{-1}$ for large ions. The small and medium-size ions increase the boundary layer's electric conductivity while the large ones, if their concentration is high enough, will essentially decrease it. So one can imagine the chain of processes in the form of flow-chart diagram presented in Figure 5. Concentration of ions depends on the ionization rate, but also on the losses connected with weather condition and recombination. The size of growing ions due to nucleation process depends on ion concentration, relative humidity as factors of formation, and weather conditions, turbulent diffusion and electric field, which can remove ions from the area of formation and growth. All these external conditions are taken into account by the introduction of chemical potential correction value ΔU. Looking at diagram in Figure 5, we can conclude that ΔU condition is a branch point. Starting from specific critical value it changes the state of atmospheric electricity and variations in ionosphere by 180° (increased/decreased air conductivity, and positive/negative plasma concentration variation in ionosphere). It was explained earlier in Pulinets (2009), and confirmed experimentally in Pulinets and Ouzounov (2011).

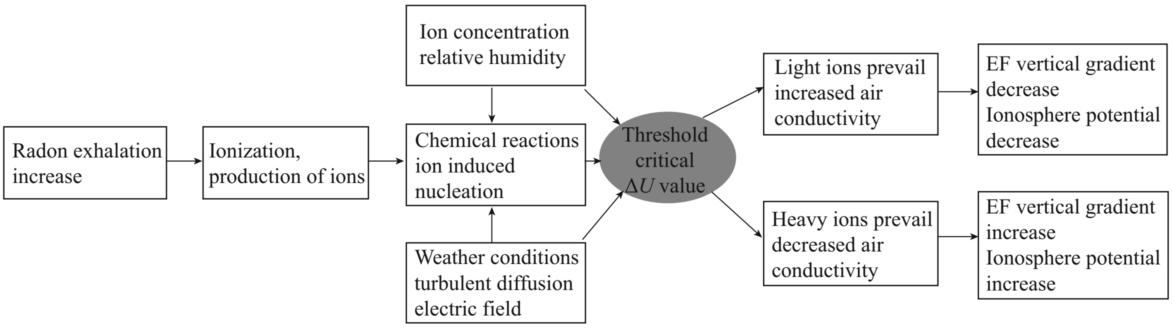

Figure 5 Flow chart of subsystems interaction with the branching point (oval).

According to Boyarchuk et al. (2010) the ΔU can be expressed in terms of usual meteorological parameters: ground air temperature $T_{\rm g}$ and relative humidity H:

$$\Delta U(\text{eV}) = 5.8 \times 10^{-10}(20\,T_{\rm g} + 5\,463)^2 \ln(100/H). \quad (3)$$

Statistical data processing for several major earthquakes during the recent five years (Boyarchuk et al., 2010) did not reveal the absolute value of the critical meaning for ΔU: it is different for different locations and probably is strongly dependent on meteorological and orography conditions. But dependence of ΔU on the distance to epicenter was revealed, which permits to determine the epicenter position with accuracy of few tens of km (depending on density of meteorological stations). Such dependence for Wenchuan earthquake is demonstrated in Figure 6.

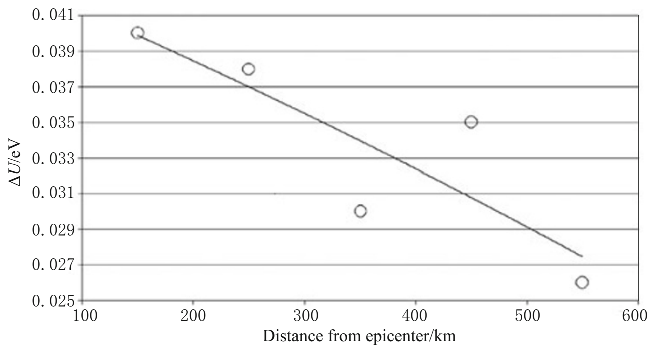

Figure 6 Chemical potential correction value ΔU dependence on the distance from the epicenter of Wenchuan earthquake (after Boyarchuk et al., 2010).

Next example of the subsystems interaction is demonstration of the nonlinear multi-scale processes in formation of the thermal anomalies. As it was demonstrated in Pulinets and Ouzounov (2011), due to more intensive radon release over active tectonic faults the land surface temperature (LST) increases mostly over the faults what gives opportunity to monitor the fault structure from satellites. This effect is registered regularly practically for all strong earthquakes with M>6. Examples of LST distribution before the Wenchuan earthquake for 1 and 5 of May 2008 are shown in Figure 7 (Huang et al., 2008). The temperature difference (within the range 2–5 °C) between the heated air over the fault and air between the faults creates the advection air movement. Simultaneously heated air creates the vertical convection flux. Both horizontal and vertical movements in the presence of Coriolis force produce condition for the formation of helical structures like it happens during formation of typhoons. Small vortices forming near ground surface are merging into larger structure like it is shown in Figure 8 (Meunier et al., 2005). Possibility of vortices emerging, persistence, and merging were considered in McWilliams (1984). This behavior is also found in the temporal evolution of spherical harmonics of the geomagnetic field (De Santis et al., 2003). Such process is called reverse cascade turbulence. It leads to the negative turbulent diffusivity and viscosity and merging of small-scale helical structures close to the ground level into the large-scale thermal spot at the top of the cloud level (Levina et al., 2000).

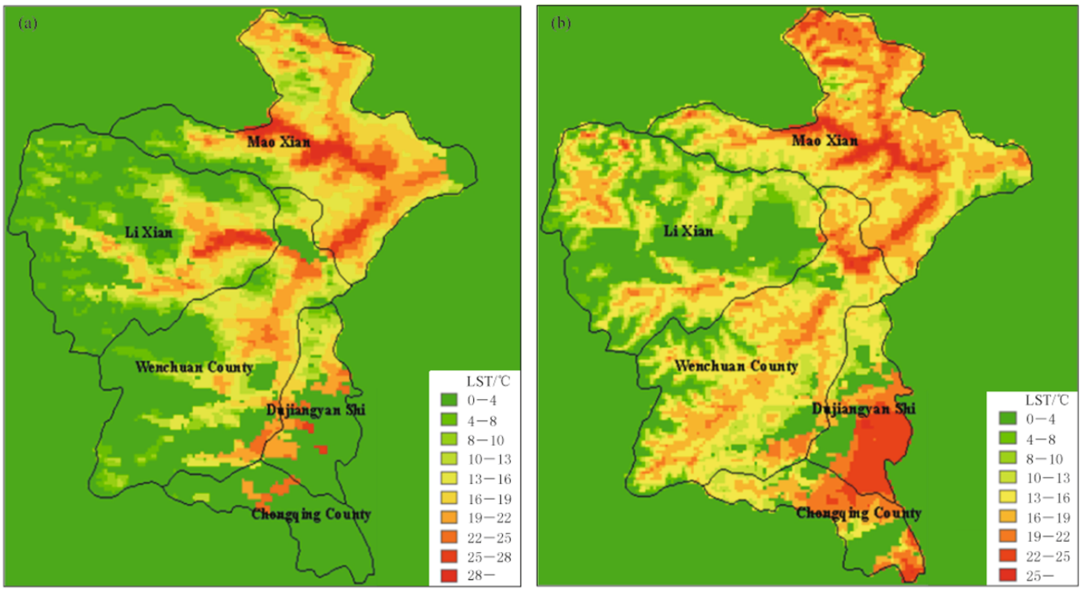

Figure 7 Land surface temperature (LST) map registered by MODIS/Terra on May 1, 2008 (a) and on May 5, 2008 (b).

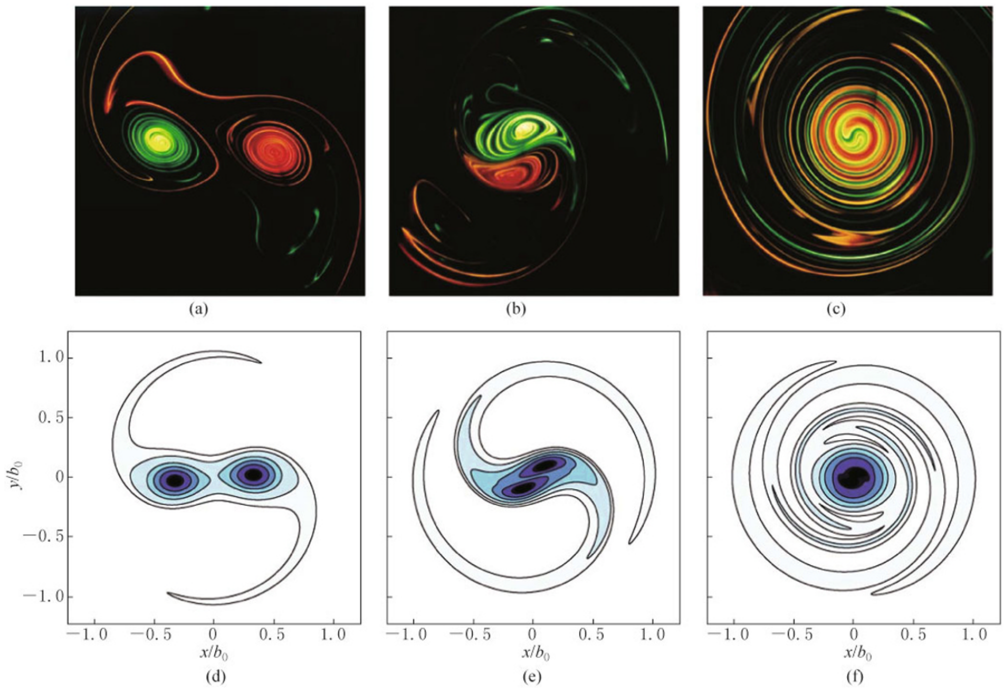

Figure 8 Examples of computer modeling of the merging vortices. (a–c) Cross-cut experimental dye visualizations of two laminar co-rotating vortices, and (d–f) vorticity fields obtained by two-dimensional direct numerical simulations. The snapshots are taken before (a, d), during (b, e) and after (c, f) merging. After Meunier et al. (2005).

The similar two and three vortices structure we can observe at higher levels (in the middle atmosphere) in the images of the surface latent heat (Li et al., 2011), see Figure 9. And the final stage is formation of the large spot at the top of atmosphere in the form of long-wave (8–14 μ) radiation (OLR). OLR registered before Wenchuan earthquake is shown in Figure 10 (Ouzounov and Pulinets, 2010).

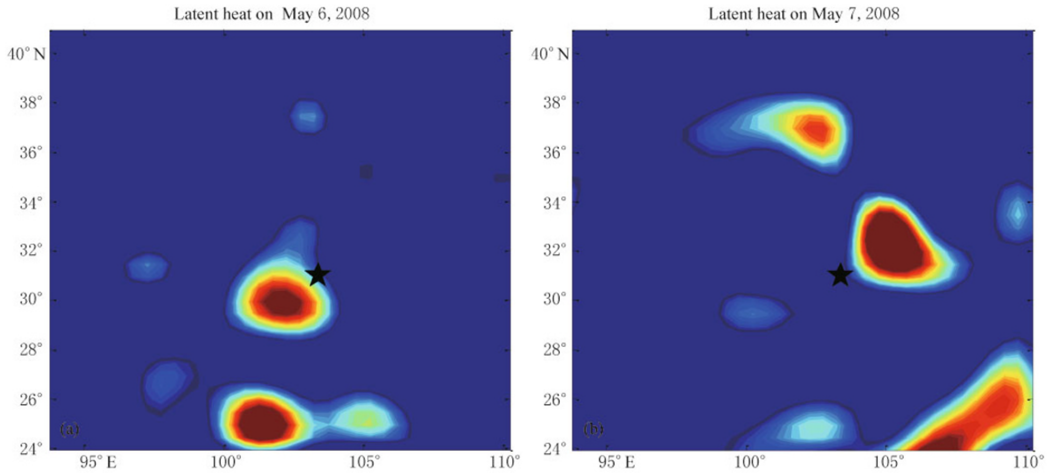

Figure 9 Latent heat flux spatial distribution registered on May 6, 2008 (a) and May 7, 2008 (b) before the Wenchuan earthquake (After Li et al., 2011).

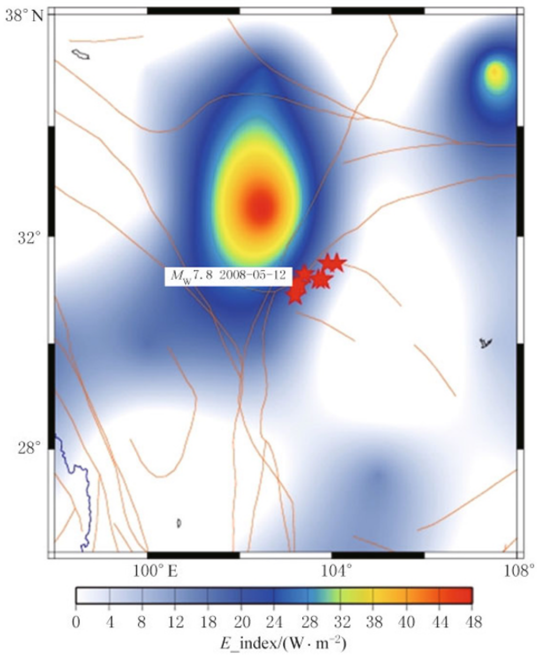

Figure 10 OLR spot registered by AVHRR/NOAA-16 satellite on May 6, 2008 (After Ouzounov and Pulinets, 2010).

The last example of the inter-geospheres interaction shows that the complete cycle of precursory information passes from atmosphere up to the ionosphere and magnetosphere, finally ends by energetic particle precipitation down to atmosphere. This chain of processes is presented in the form of ring diagram (Figure 11), and is described in Pulinets et al. (2002) and Kim et al. (2002). The anomalies of atmospheric electricity (mainly through the modification of air conductivity) create the large-scale irregularities in ionosphere. Because of high conductivity of geomagnetic field lines, the magnetospheric tube leaned onto the modified region of the ionosphere becomes to be modified through formation of field aligned electron density irregularities (this feature is a cause of magnetically conjugated effects observed in ionospheric precursors of earthquakes records, especially for low-latitude earthquakes). The VLF noises due to existence of plasma irregularities are scattered into the modified magnetospheric tube (Shklyar and Nagano, 1998), which creates the increased level of VLF emissions within the modified tube (Larkina et al., 1983). Natural incoherent wideband VLF radiation trapped in a magnetospheric duct should lead to chaotic variations in the pitch angles of energetic electrons. Mathematically, such a pitch-angle scattering can be described as diffusion in the pitch-angle space (Roberts, 1969). Interaction of electrons of radiation belt with VLF emission in the case of earthquakes is similar to interaction of lightning-induced whistler VLF emission with electrons (Strangeways, 1999) but has its own features (Anagnostopoulos et al., 2011). Not only precipitating electrons are observed but also the protons. This mechanism was considered by Shklyar (1986). The

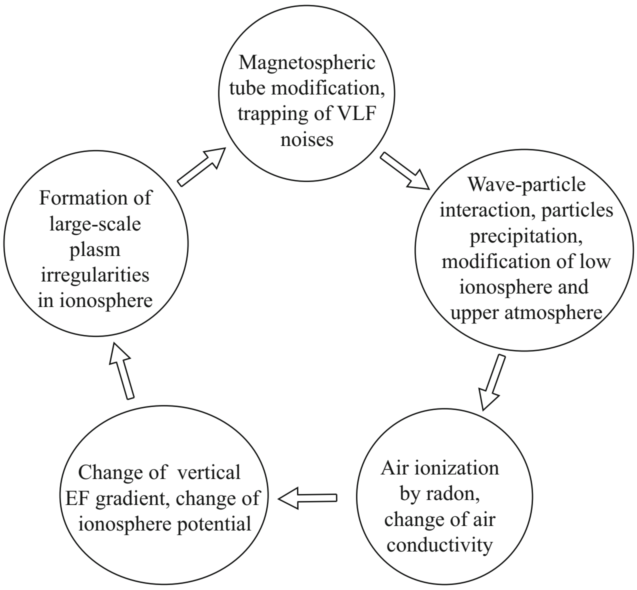

Figure 11 Ring-type action of LAIC: atmospheric effects from below and from above.

relaxation of energetic particles after precipitation leads to increased ionization of the lower ionosphere (D-region) and upper atmosphere (Paulikas, 1975), closing the ring of interactions.

The purpose of this paragraph was to demonstrate that the set of geophysical anomalies observed at different levels from the ground surface up to magnetosphere is not a set of individual independent processes, but it is a complex system of processes, which could be subdivided by subsystems interacting with each other. It is a nonlinear system with multi-variant results of interaction having different level thresholds determining the further development. Every subsystem takes part in several interactions simultaneously, and precursor development has direction of system state development and disturbance propagation from the bottom to upper layers of atmosphere and ionosphere: every previous precursor supports development of the next one — it is a kind of “cooperation” which was named by Herman Haken as synergetics (Haken, 2004).

4 LAIC model as an open system

Theoretical estimations and experimental data for more than hundred of recent strong earthquakes happened during the last decade have demonstrated that enormous amounts of thermal energy are released before earthquakes (Kafatos et al., 2007; Ouzounov et al., 2007; Li et al., 2011). Before Sumatra $M9.3$ earthquake latent heat anomalies of $\sim$100 W$\cdot$m^{-2} persisting for 10 days, over nine, 200 km$\times$200 km grids released 3.1×10^{19} J which is almost an order of magnitude larger than mechanical energy released during the main rupture (4.3×10^{18} J) (Kafatos et al., 2007). Also reported is the surface air temperature increase over the area of hundreds thousand square kilometers (Mil’kis, 1986; Dunajecka and Pulinets, 2005). The anomalies of outgoing longwave radiation (OLR) are reported with energy fluxes from 10 to 200 W$\cdot$m^2 (Ouzonov et al., 2006, 2007; Li et al., 2011). The question appears: are relatively weak radon fluxes (even over large territory) able to produce such a huge amount of energy? And here we come to the most important point of the LAIC kernel: radon does not produce energy, it produces the ions — centers for water vapor condensation, and condensation itself is the source of the thermal energy. Actually, we can say that radon produces the heterogeneous catalysis reaction, changing the relation between two phases of the water state with release of the latent heat, because our reaction (condensation) proceeds with the energy release. How strong is change of phase state relation? Laakso et al. (2003) have demonstrated that condensation enhancement take place due to Coulomb interaction between the ions and water molecules, and this enhancement is near 5-fold. Svensmark et al. (2007) demonstrated in laboratory experiments that nucleation rate is proportional to the ion density.

And still the question remains: where is the source of energy? The answer is very simple: it is Sun. Thermal energy in the form of latent heat is in the water vapor which was created earlier in the normal daily cycle of latent heat transformation. So, our system dips out the energy from environment, and in this point we can determine it as pure open system.

5 Critical point/instant or critical time interval?

The last point in the discussion on the LAIC properties is the question, when does the system reach the critical point? In the first paragraph (see Figure 1) the critical point moment was determined by the best fitting to the power-law time-to-failure equation, and finally the value 1995.045 (17 January) day of earthquake was obtained (Yasuoka et al., 2009). But with different selection of initial parameters this value varied from 1995.034 (13 January) to 1995.073 (27 January), which gives some interval of uncertainty.

The entropy concept was developed by De Santis et al. (2011) to demonstrate the system approach towards the critical point with two examples of earthquakes in Italy. According to their analysis the critical point (entropy maximum) is reached 5 hours after the main shock, and the main shock belongs to an ensemble of earthquakes that occur some time before it and ends a short time after (Figure 12) where entropy development was estimated by two methods: 200-event adjacent nonoverlaping windows (Figure 12a), and entropy estimated over 200-event moving windows (Figure 12b).

Analysis revealed the threshold in entropy value H_t=0.1 which can be interpreted as the point of no reverse when the system moves one-way to the main fault rupture. In case of L'Aquila earthquake this values was reached on 30 of March with the largest foreshock (M_L4.1). We can interpret the interval between the 30 of March and moment when entropy maximum was reached as period of short-term precursors because the system entered the way with no return.

We should underline the striking coincidence of the period determined by De Santis et al. (2011) with period of different anomalies registered before L'Aquila earthquake and reported in different publications (Rozhnoi et al., 2009; Ouzounov et al., 2011). In Figure 13 the anomaly of VLF signal amplitude for sub-ionospheric propagation over the earthquake epicenter is presented. One can clearly see that anomaly started on 31 of March after crossing the system of the critical level. The same situation is observed for ground temperature, OLR and ionospheric anomalies reported in Ouzounov et al. (2011).

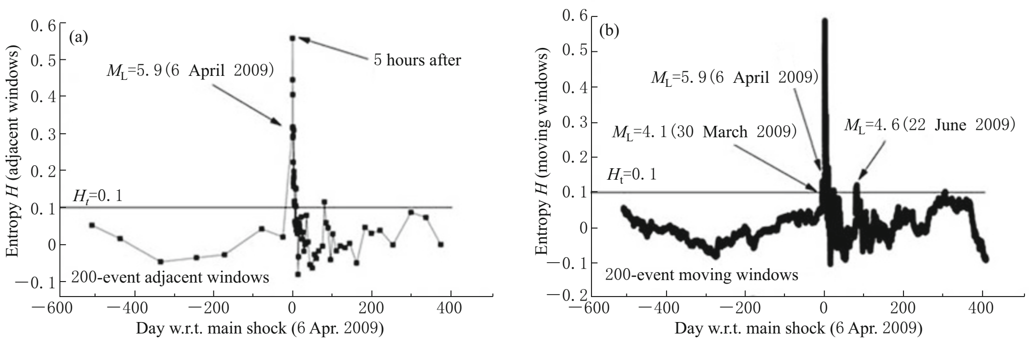

Figure 12 Entropy dynamics for L'Aquila earthquake of 6 April 2009. (a) Calculation for nonadjacent windows; (b) Calculation for moving windows (after De Santis et al., 2011).

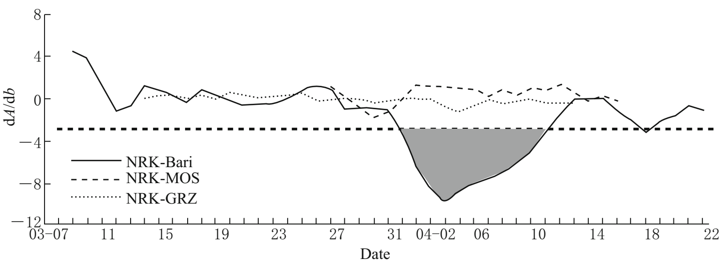

Figure 13 Solid curve presents the night-time residual amplitude of the VLF signal for the pass NRK-Bari passing over epicenter of L'Aquila earthquake. Shadowed area means signal crossing the 2σ level. Dotted and dashed lines present signal for passes NRK-GRZ and NRK-MOS which not pass over epicenter area (after Rozhnoi et al., 2009).

This example let us to claim once more that anomalies stimulated by radon exhalation before earthquakes and described in LAIC are the real short-term earthquake precursors.

The only question remains, which seismologists consider very important and which was not answered in the present paper discussing the physical precursors is: where is the co-seismic signal? The answer again is not very complex. Atmospheric and ionospheric precursors are generated not directly by crust deformations, but by radon release. Through their temporal dynamics they carry information on earthquake preparation transmitted by radon, and their development is determined by the time constants of plasma chemical reactions, and delayed reaction of meteorological parameters. The majority of atmospheric processes do not react immediately, nevertheless their development before earthquakes also has character of critical process, and their spatial and temporal distributions are determined by the earthquake preparation zone (earthquake magnitude) and radon variation dynamics described by the power law indicating time-to-failure.

Recently the ionospheric anomaly was detected which probably has direct connection with the rupture process and could be regarded as co-seismic. It is GPS TEC enhancement, which lasts near 1 hour and centered at the main shock time. But it is observed only for the mega-earthquakes with magnitude close to 9 and one of the possible mechanisms is the triboelectricity when the pre-rupture slipping process starts (Heki, 2011). At present moment we can state that it is just discovered phenomena, and its physical mechanism study is before us.

6 Conclusions

This paper was devoted to discussion of LAIC model not in the sense of its description (what is done elsewhere: Pulinets and Ouzounov, 2011) but to deeper understanding its qualities from the point of view of complexity and synergy of precursors described by model. It was demonstrated that radon still remains the earthquake precursor both from point of view formal seismological definition and from physical point of view. It also attempts to demonstrate that the LAIC as a complex system being a derivative from intensive radon activity before earthquakes starts to demonstrate anomalies in atmosphere, ionosphere and magnetosphere only when the system approaches the critical state which in turn can be determined by the threshold value of the system entropy. This conception opens the way to merge seismological and physical approaches to determination of short-term earthquake precursors.

Acknowledgements Author would like to thank Institute of Seismology and Volcanology of Hokkaido University, whose creative atmosphere inspired the author to write this paper during his stay in the institute as invited professor. The research leading to these results has received funding from the European Union Seventh Framework Program (FP7/20017-2013) under grant agreement No. 263502 – – PRE-EARTHQUAKES project: Processing Russian and European EARTH observations for earthquake precursors studies. The document reflects only the author's views and the European Union is not liable for any use that may be made of the information contained herein.

References

Aki K and Richards P G (1980). *Quantitative Seismology. Theory and Methods*. Freeman, New York, 930pp.

Anagnostopoulos G, Rigas V and Vassiliadis E (2011). Radiation belt electron precipitation in the upper ionosphere at middle latitudes before strong earthquakes. http://arxiv.org/abs/1012.3588v1.

Aumento F (2002). Radon tides on an active volcanic island (Terceira, Azores). *Geofsica Internacional* **41**(4): 499–505.

Ben-Zion Y and Lyakhovsky V (2002). Accelerated seismic release and related aspects of seismicity patterns on earthquake faults. *Pure Appl Geophys* **159**: 2 385–2 412.

Bowman D D, Ouillon G, Sammis C G, Sornette A and Sornette D (1998). An observational test of the critical earthquake concept. *J Geophys Res* **103**: 24 358–24 372.

Boyarchuk K A, Karelin A V and Nadolski A V (2010). Statistical analysis of the chemical potential correction value of the water vapor in atmosphere on the distance from earthquake epicenter. *The Issues of Electromechanics* **116**: 39–46.

Cicerone R D, Engel J E and Britton J (2009). A systematic compilation of earthquake precursors. *Tectonophysics* **476**: 371–396.

Das N K, Bhandari R K, Ghose D, Sen P and Sinha B (2005). Anomalous fluctuation of radon, gamma dose and helium emanating from a thermal spring prior to an earthquake. *Current Science* **89**: 1 399–1 404.

De Santis A (2009). Geosystemics. *Proceedings of the 3rd IASME/WSEAS International Conference on Geology and Seismology* (GES'09). Feb. 23–26, 2009, Cambridge, 36–40.

De Santis A, Barraclough D R and Tozzi R (2003). Spatial and temporal spectra of the geomagnetic field and their scaling properties. *Physics Earth Planet Inter* **135**: 125–134.

De Santis A, Cianchini G, Qamili E and Frepoli A (2010). The 2009 L'Aquila (Central Italy) seismic sequence as a chaotic process. *Tectonophysics* **496**: 44–52.

De Santis A, Cianchini G, Favali P, Beranzoli L and Boschi E (2011). The Gutenberg-Richter law and entropy of earthquakes: Two case studies in Central Italy. *Bull Seismol Soc Am* **101**: 1 386–1 395.

Dobrovolsky I P (2009). *Mathematical Theory of the Tectonic Earthquake Preparation and Prediction*. Fizmatlit, Moscow, 236pp (in Russian).

Dobrovolsky I P, Zubkov S I and Myachkin V I (1979). Estimation of the size of earthquake preparation zones. *Pure Appl Geophys* **117**: 1 025–1 044.

Dunajecka M and Pulinets S A (2005). Atmospheric and thermal anomalies observed around the time of strong earthquakes in Mexico. *Atmosfera* **18**: 233–247.

Eddington A (1928). *The Nature of the Physical World*. Cambridge University Press, Cambridge, 361pp.

Fleischer R L (1981). Dislocation model for radon response to distant earthquakes. *Geophys Res Lett* **8**: 477–480.

Geller R J, Jackson D D, Kagan Y Y and Mulargia F (1997). Earthquakes cannot be predicted. *Science* **275**: 1 616–1 618.

Haken H (2004). *Synergetics. Introduction and Advanced Topics*. Springer-Verlag, Berlin, Heidelberg, 755pp.

Heki K (2011). Ionospheric electron enhancement preceding the 2011 Tohoku-Oki earthquake. *Geophys Res Lett* **38**: L17312, doi:10.1029/2011GL047908.

Hirsikko A (2011). *On Formation, Growth and Concentrations of Air Ions*. Report series of aerosol science No. 125, Helsinki Universtiy, 64pp.

Hõrrak U (2001). *Air Ion Mobility Spectrum at a Rural Area*. [Ph.D. Dissertation]. Institute of Environmental Physics, University of Tartu, Tartu, Estonia, 81pp.

Hõrrak U, Mirme A, Salm J, Tamm E and Tammet H (1998). Air ion measurements as a source of information about atmospheric aerosols. *Atmospheric Research* **46**: 233–242.

Huang J, Mao F, Zhou W and Zhu X (2008). Satellite thermal IR associated with Wenchuan earthquake in China using MODIS data. *Proceeding of the 14th World Conference on Earthquake Engineering*. October 12–17, 2008, Beijing, China.

İnan S, Akgül T, Seyis C, Saatçılar R, Baykut S, Ergintav S and Baş M (2008). Geochemical monitoring in the Marmara region (NW Turkey): A search for precursors of seismic activity. *J Geophys Res* **113**: B03401, doi:10.1029/2007JB005206.

Kafatos M, Ouzounov D, Pulinets S, Cervone G and Singh R (2007). Energies associated with the Sumatra earthquakes of December 26, 2004 and March 28, 2005. *AGU* 2007 *Fall Meeting*. San Francisco, paper S42B-04.

Kanamori H and Anderson D L (1975). Theoretical basis of some empirical relations in seismology. *Bull Seismol Soc Am* **65**: 1 073–1 095.

Kim V P, Pulinets S A and Hegai V V (2002). Theoretical model of possible disturbances in the nighttime midlatitude ionospheric D-region over an area of strong-earthquake preparation. *Radiophysics and Quantum Radioelectronics* **45**: 262–268.

Kondepudi D and Prigogine I (1998). *Modern Thermodynamics: From Heat Engines to Dissipative Structures*. Wiley & Blackwell, Chichester, New York, 508pp.

Laakso L, Kulmala M and Lehtinen K E J (2003). Effect of condensation rate enhancement factor on 3-nm (diameter) particle formation in binary ion-induced and homogeneous nucleation. *J Geophys Res* **108**(D18): 4 574, doi:10.1029/2003JD003432.

Laakso L, Mäkelä J M, Pirjola L and Kulmala M (2002). Model studies on ion-induced nucleation in the atmosphere. *J Geophys Res* **107**(D20): 4 427, doi:10.1029/2002JD002140.

Larkina V I, Migulin V V, Nalivaiko A V, Gershenzon N I, Gokhberg M B, Liperovsky V A and Shalimov S L (1983). Observation of VLF emissions, related with seismic activity, on the Intercosmos-19 satellite. *Geomagnetism and Aeronomy* **23**: 684–687.

Levina G V, Moiseev S S and Rutkevich P B (2000). Hydrodynamic alpha-effect in a convective system. In: Debnath L and Riahi D N eds. *Series: Advances in Fluid Mechanics. Nonlinear Instability, Chaos and Turbulence*. WIT Press, Southampton, Boston, (2): 111–162.

Li K C, Feng J, Pan X and Qu C Y (2011). Application of multi-parameter infrared remote sensing in seismic monitoring. *International Workshop of Earthquake Anomaly Recognition*. September 18–20, 2011, Northeastern University, Shenyang, China.

McWilliams J C (1984). The emergence of isolated coherent vortices in turbulent flow. *J Fluid Mech* **146**: 21–43.

Meunier P, Le Dizès S and Leweke T (2005). Physics of vortex merging. *Comptes Rendus Physique* **6**: 431–450.

Mil'kis M R (1986). Meteorological precursors of earthquakes. *Izvestiya, Earth Physics* **22**: 195–204.

Ouzounov D, Bryant N, Logan T, Pulinets S and Taylor P (2006). Satellite thermal IR phenomena associated with some of the major earthquakes in 1999–2003. *Phys Chem Earth* **31**: 154–163.

Ouzounov D, Liu D, Chunli K, Cervone G, Kafatos M and Taylor P (2007). Outgoing long wave radiation variability from IR satellite data prior to major earthquakes. *Tectonophysics* **431**: 211–220.

Ouzounov D and Pulinets S (2010). Interdisplinary approach of validating atmospheric signals associated with major earthquakes. *The Top Seminar for RS Application in Earthquake Monitoring and Earthquake-Related Satellite Missions*. 6–8 September, 2010, Beijing, China.

Ouzounov D, Pulinets S, Cervone G, Kafatos M, Parrot M and Taylor P (2005). Progress in understanding the EM phenomena related to major earthquakes by analyzing multisensor satellite and ground data. *EMSEV Workshop*. Nov. 3–4, 2005, Puerto Vallarta, Mexico.

Ouzounov D, Pulinets S, Giuliani G, Fioravanti G, Ciraolo L, Kafatos M and Taylor P (2011). Atmosphere awakening prior to M6.3 earthquake of April 6, 2009 revealed by joined analysis of satellite and in-situ data. *Nat Hazards Earth Syst Sci* (submitted)

Paulikas G A (1975). Precipitation of particles at low and middle latitudes. *Rev Geophys* **13**: 709–734.

Pulinets S and Ouzounov D (2011). Lithosphere-Atmosphere-Ionosphere Coupling (LAIC) model — an unified concept for earthquake precursors validation. *J*

Asian Earth Sci **41**: 371–382.

Pulinets S A (2009). Physical mechanism of the vertical electric field generation over active tectonic faults. *Advances in Space Research* **44**: 767–773.

Pulinets S A and Boyarchuk K A (2004). *Ionospheric Precursors of Earthquakes*. Springer, Berlin, 315pp.

Pulinets S A, Boyarchuk K A, Hegai V V, Kim V P and Lomonosov A M (2000). Quasielectrostatic model of atmosphere-thermosphere-ionosphere coupling. *Adv Space Res* **26**: 1 209–1 218.

Pulinets S A, Boyarchuk K A, Hegai V V and Karelin A V (2002). Conception and model of seismo-ionosphere-magnetosphere coupling. In: Hayakawa M and Molchanov O A eds. *Seismo-Electromagnetics*: *Lithosphere-Atmosphere-Ionosphere Coupling*. TERRAPUB, Tokyo, 353–361.

Pulinets S A, Khegai V V, Boyarchuk K A and Lomonosov A M (1998). Atmospheric electric field as a source of ionospheric variability. *Physics-Uspekhi* **41**: 515–522.

Pulinets S A, Liu J Y and Safronova I A (2004). Interpretation of a statistical analysis of variations in the foF2 critical frequency before earthquakes based on data from Chung-Li ionospheric station (Taiwan). *Geomagnetism and Aeronomy* **44**(1): 102–106.

Pulinets S A, Ouzounov D, Karelin A V, Boyarchuk K A and Pokhmelnykh L A (2006). The physical nature of the thermal anomalies observed before strong earthquakes. *Phys Chem Earth* **31**: 143–153.

Roberts C S (1969). Pitch-angle diffusion of electrons in the magnetosphere. *Rev Geophys* **7**: 305–337.

Roelofs E (1998). Radon and rocks deformations. *Nature* **399**: 104–105.

Rozhnoi A, Solovieva M, Molchanov O, Schwingenschuh K, Boudjada M, Biagi P F, Maggipinto T, Castellana L, Ermini A and Hayakawa M (2009). Anomalies in VLF radio signals prior the Abruzzo earthquake (M=6.3) on 6 April 2009. *Nat Hazards Earth Syst Sci* **9**: 1 727–1 732.

Scholz C H, Sykes L R and Aggarwal Y P (1973). Earthquake prediction: A physical basis. *Science* **181**: 803–809.

Šebela S, Vaupotič J, Košťák B and Stemberk J (2010). Direct measurement of present-day tectonic movement and associated radon flux in Postojna Cave, Slovenia. *Journal of Cave and Karst Studies* **72**: 21–34, doi:10.4311/jcks2009es0077.

Sekimoto K and Takayama M (2007). Influence of needle voltage on the formation of negative core ions using atmospheric pressure corona discharge in air. *International Journal of Mass Spectrometry* **261**: 38–44.

Shklyar D R (1986). Particle interaction with an electrostatic VLF wave in the magnetosphere with an application to proton precipitation. *Planetary and Space Science* **34**: 1 091–1 099.

Shklyar D R and Nagano I (1998). On VLF wave scattering in plasma with density irregularities. *J Geophys Res* **103**: 29 515–29 526.

Sornette D and Sammis C G (1995). Complex critical exponents from renormalization group theory of earthquakes: implications for earthquake predictions. *J Phys I France* **5**: 607–619.

Strangeways S J (1999). Lightning induced enhancements of D-region ionization and whistler ducts. *Journal of Atmospheric and Solar-Terrestrial Physics* **61**: 1 067–1 080.

Svensmark H, Pedersen J O P, Marsch N D, Enghoff M B and Uggerhφj U I (2007). Experimental evidence for the role of ions in particle nucleation under atmospheric conditions. *Proc R Soc A* **463**: 385–396.

Thacker B H, Doebling S W, Hemez F M, Anderson M C, Pepin J E, Rodriguez E A (2004). *Concepts of Model Verification and Validation*. Report No. LA-14167-MS, Los Alamos National Laboratory.

Toutain J-P and Baubron J-C (1998). Gas geochemistry and seismotectonics: a review. *Tectonophysics* **304**: 1–27.

Triqué M, Richon P, Perrier F, Avouac J P, Sabroux J C (1999). Radon emanation and electric potential variations associated with transient deformation near reservoir lakes. *Nature* **399**: 137–141.

Wyss M (1997a). Cannot earthquakes be predicted? *Science* **278**: 487–488.

Wyss M (1997b). Second round of evaluations of proposed earthquake precursors. *Pure Appl Geophys* **149**: 3–16.

Yasuoka Y, Igarashi G, Ishikawa T, Tokonami S and Shinogi M (2006). Evidence of precursor phenomena in the Kobe earthquake obtained from atmospheric radon concentration. *Applied Geochemistry* **21**: 1 064–1 072.

Yasuoka Y, Kawada Y, Nagahama H, Omori Y, Ishikawa T, Tokonami S and Shinogi M (2009). Preseismic changes in atmospheric radon concentration and crustal strain. *Phys Chem Earth* **34**: 431–434.

Yasuoka Y, Nagahama H and Ishikawa T (2010). *Anomalous Radon Concentration Prior to an Earthquake*: *A Case Study on the* 1995 *Kobe Earthquake*, *Japan*. Lambert Academic Publishing, Saarbrücken, Germany, 138pp.

Yu F and Turco R P (2001). From molecular clusters to nanoparticles: The role of ambient ionization in tropospheric aerosol formation. *J Geophys Res* **106**: 4 797–4 814.